Article

Assessment of Lightweight Concrete Thermal Properties at Elevated Temperatures

Juan Enrique Martínez-Martínez [1,*] , **Felipe Pedro Álvarez Rabanal** [1] , **Mariano Lázaro** [2] ,
Mar Alonso-Martínez [1] , **Daniel Alvear** [3] **and Juan José del Coz-Díaz** [1]

1   GICONSIME Research Group, University of Oviedo, 33204 Gijón, Spain; felipe@constru.uniovi.es (F.P.Á.R.);
     mar@constru.uniovi.es (M.A.-M.); juanjo@constru.uniovi.es (J.J.d.C.-D.)
2   GIDAI Research Group, University of Cantabria, 39005 Santander, Spain; mariano.lazaro@unican.es
3   Dirección General de Industria, Energía y Minas, Gobierno de Cantabria, 39011 Santander, Spain;
     alveard@unican.es
*   Correspondence: quique@constru.uniovi.es

Abstract: Structural lightweight concrete (LWC) has recently acquired research importance because of its good thermal insulation properties. However, there is a lack of knowledge about its thermal properties at elevated temperatures. The thermal properties, such as thermal conductivity and specific heat, of porous LWC vary depending on the aggregates, air voids, and moisture content of the LWC in question. To study these effects, in this paper, we measured the thermal properties of three types of structural LWCs at different temperatures, combining different characterization techniques, namely, differential scanning calorimetry (DSC), laser flash analysis (LFA), and modified transient plane source (MTPS). Bulk density and porosity were also evaluated. Specific heat is analyzed by the DSC technique from 20 to 1000 °C and the MTPS technique from 20 to 160 °C. Thermal conductivity is studied using MTPS and LFA techniques at temperatures ranging from 20 to 160 °C and 100 to 300 °C, respectively. The results indicate that the thermal properties of LWC are highly affected by moisture content, temperature, and porosity. For LWC, the current Eurocodes 2 and 4 assume a constant value of specific heat (840 J/kg°C). This research reveals variability in temperatures near 150, 450, and 850 °C due to endothermic reactions. Furthermore, for low temperatures, the higher the porosity, the higher the thermal conductivity, while, at high temperatures, the higher the porosity, the lower the thermal conductivity. Thus, Eurocodes 2 and 4 should be updated accordingly. This research contributes to a deeper understanding and more accurate prediction of LWC's effects on thermal properties at elevated temperatures.

Keywords: lightweight concrete; thermal conductivity; specific heat; elevated temperatures

1. Introduction

Concrete is widely used as a primary structural material in construction due to its numerous advantages, such as strength, durability, ease of fabrication, and non-combustibility [1]. Concrete is grouped into different categories based on performance (conventional and high performance), weight (normal weight and lightweight), presence of aggregates (fibers, waste materials, and recycles aggregate concrete) [2–4], and strength (normal strength, high strength, and ultra-high strength).

According to the International Energy Agency (IEA), the current demand for energy is 30% higher than it was in the 1990s [5]. Improving the thermal properties of concrete can significantly reduce heat loss in buildings and improve sustainability. Lightweight concrete (LWC) has been extensively used as both a structural and non-structural building material due to its important advantages, including a longer product life cycle than other construction materials. This type of concrete has low density, excellent behavior at elevated temperatures, and good thermal insulation due to its low thermal conductivity [6–8]. LWC is usually manufactured using lightweight aggregates such as perlite, pumice, vermiculite,

or expanded clay [1,9]. Recently, to mitigate some of concrete's environmental problems, LWC has also been manufactured using waste from different industries, such as fly ash and blast furnace slag, to substitute components and/or enhance the concrete's properties [10].

Fire is a severe environmental condition to which structures may be subjected. The behavior of a concrete element exposed to elevated temperature depends on its thermal and mechanical properties. The main thermal properties that influence temperature rises and distributions in concrete are thermal conductivity and specific heat. Previous experimental studies have reported that the thermal properties of concrete are highly influenced by aggregate type, moisture content, and porosity, as well as the composition of the concrete mix [4,11–16].

The thermal conductivity of normal concrete (NC) at ambient ranges is from 1.36 to 2 W/mK according to EN 1992-1-2 [17] and the standard EN 1994-1-2 [18]. Overall thermal conductivity, as well as the density of concrete, decrease with temperature. This trend is usually attributed to variations in moisture content with temperature [19]. The water contained within concrete starts to evaporate between 100 and 120 °C. Subsequently, the dissociation of the water of the hydrated calcium silicate (C-S-H) occurs between 150 and 400 °C. Finally, loss of mass occurs between 400 and 600 °C, weakening the concrete. The value of thermal conductivity may vary depending on the measurement method used [4]. Usually, homogeneous materials are studied using steady-state methods, such as the guarded hot plate method and laser flash analysis (LFA). Although these methods take more time, the values they achieve are more accurate than those achieved with transient methods. Transient methods are used for heterogeneous materials such as concrete. In addition, transient methods have some advantages, such as an easy and fast measurement procedure, the possibility of measuring different thermal properties simultaneously, and the absence of a calibration sample. Transient methods such as a transient plane source are usually favored for wet concrete due to its changes at elevated temperatures [4,14,20]. However, there is no discussion in the literature about the selection of a proper method for measuring thermal conductivity.

The specific heat of NC at ambient temperatures ranges from 840 to 1800 J/kg·K [1]. Specific heat is sensitive to various physical and chemical transformations that take place in concrete at elevated temperatures. During heating, free water vaporizes between 90 and 120 °C [4,12,21]. Between 180 and 300 °C, the loss of chemically bonded water occurs. Between 400 and 600 °C, there is a dissociation of calcium hydroxide ($Ca(OH)_2$) into calcium oxide (CaO) and water (H_2O). At this point, there is a complete desiccation of the pore system. From this point on, the gradual mass loss is attributed to the release of carbon dioxide (CO_2) from calcium carbonate ($CaCO_3$) [22]. Therefore, specific heat is highly dependent on free water content. It is usually measured by means of differential scanning calorimetry (DSC) or differential thermal analysis (DTA) for temperatures above 600 °C [1].

Most research on LWC shows a significant variation in the thermal properties, which are affected by the fraction of lightweight aggregates and density [7,23]. The addition of regular aggregates facilitates heat conduction. The introduction of internal pores affects thermal behavior, increasing the absorption of water into the lightweight aggregate and delaying the dehydration of the calcium hydroxide [4]. However, the standard EN 1992-1-2 [17] and the standard EN 1994-1-2 [18], hereafter referred to Eurocode 2 and Eurocode 4, respectively, set a constant value for specific heat of 840 J/(kg·K) for any LWC, as well as a linear variation in thermal conductivity in the range of 20–800 °C.

According to the literature, there are many studies on lightweight aggregates and their usage in lightweight systems. However, studies about the effect of elevated temperatures in LWC thermal properties are limited, and there is also limited guidance for undertaking standardized property tests at elevated temperatures [24]. Therefore, this work carries out research on the thermal conductivity and specific heat of various structural LWCs. Samples containing different proportions of aggregates are compared at ambient and elevated temperatures. To measure thermal properties, three different test methods are used: differential scanning calorimetry (DSC), laser flash analysis (LFA), and modified

transient plane source (MTPS). There are three main objectives of this research work. First, we seek to measure the specific heat (c_p) of the LWC over a wide temperature range (20–1000 °C); the measured c_p values of LWC using DSC and MTPS methods are compared. Second, we aim to study thermal conductivity (k) over a range of 20–300 °C in LWCs; for this purpose, MTPS and LFA methods are combined. Finally, we endeavor to propose a relationship between density, thermal conductivity, and temperature, as well as between specific heat and temperature.

2. Materials and Methods

2.1. Materials

Three different types of LWC were manufactured to study their thermal properties under elevated temperatures. Portland cement, siliceous aggregates, two sizes of expanded clay, water, and polyolefin fibers were used to manufacture LWC samples. Portland-composite cement of grade CEM II/A-V 42.5 was used in this study following Standard UNE-EN 197-1:2011 [25]. In addition, siliceous aggregates with a diameter of 0–2 mm, expanded clay-fine (ECF) with diameters of 1–5 mm and a density of 430 kg/m^3, and expanded clay-coarse (ECC) with diameters of 2–10 mm and a density of 350 kg/m^3 were used to manufacture the LWCs. Expanded clay is usually employed to manufacture high-performance ultra-light mortars. Its main properties are good insulation, porosity, and resistance. In order to avoid shrinkage cracking, polyolefin fibers 48 mm in length and with a density of 910 kg/m^3 were used. Figure 1 shows the types of aggregate used in this study.
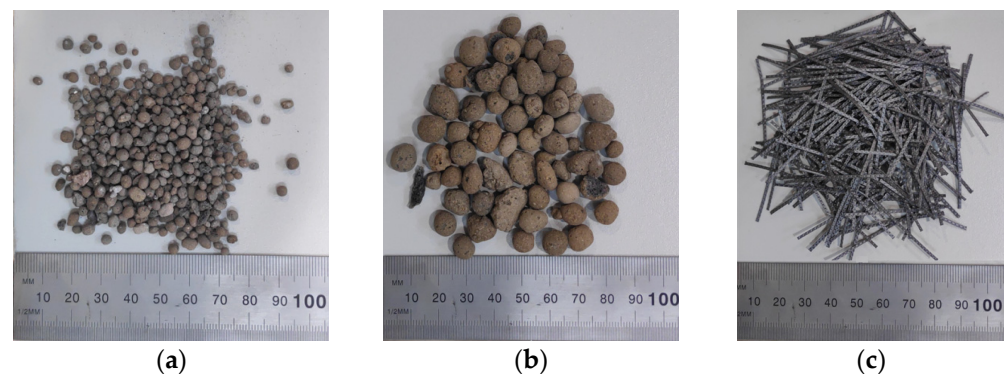
Figure 1. Types of aggregates: (**a**) expanded clay-fine; (**b**) expanded clay-coarse; (**c**) polyolefin fibers.

2.2. Mix Proportions

Following UNE 83502:2004 [26] and UNE 83504:2004 [27], twelve concrete samples were manufactured for each LWC in the laboratory. The mix proportions of expanded clay aggregates, siliceous aggregate, cement, and water are shown in Table 1. LWC-1 was prepared using 4.95 L of ECF, 6.3 L of ECC, 14.71 kg of siliceous aggregate, 11.7 kg of cement, and 5.66 L of water. LWC-2 was prepared using 5.25 L of ECF, 4.5 L of ECC, 17.11 kg of siliceous aggregate, 11.7 kg of cement, and 5.66 L of water. LWC-3 was prepared using 3.6 L of ECF, 3.6 L of ECC, 20.02 kg of siliceous aggregate, 12.6 kg of cement, and 6.09 L of water.

Table 1. Mixing proportions of lightweight concretes in mass fractions.

Mixing Compositions	Constituents				
	ECF (%)	ECC (%)	Siliceous Aggregate 0/2 (%)	Cement 42.5R (%)	Water (%)
LWC-1	5.85	6.05	40.42	32.14	15.54
LWC-2	5.89	4.11	44.68	30.55	14.77
LWC-3	3.91	4.50	44.44	31.79	15.36

LWCs have pores within their structure. In order to know their porosity, true density (ρ_{true}) and bulk density (ρ_{bulk}) were measured using dry samples [28]. The porosity (n) of the dry LWC samples was estimated using Equation (1). The true density of each LWC was measured using a helium pycnometer model AccuPyc 1340, which provided high-speed, high-precision volume measurements and density calculations. To measure the bulk density, volume, and mass, standardized cylindrical samples of $\Phi 15 \times 30$ cm were used. The results are shown in Table 2.

$$n = \left(\frac{\rho_{true} - \rho_{bulk}}{\rho_{true}} \right) \times 100\% \tag{1}$$

Table 2. Density and porosity of LWCs.

Material	Bulk Density (kg/m^3)	True Density (kg/m^3)	Porosity (%)
LWC-1	1740	2430	28.2
LWC-2	1819	2485	26.6
LWC-3	1906	2502	24

2.3. Methodology

In this work, the thermal conductivity and the specific heat of different LWCs were studied using different transient methods. The results of each method were also compared. Thermal conductivity (k) is the property of a material to conduct heat. LWC is a porous and heterogeneous material; two different methods to compare its thermal conductivity at different temperatures were used: LFA and MTPS. Specific heat (c_p) is the amount of heat per unit mass required to change the temperature of a material by one degree. This thermal property was measured using two different methods: MTPS and DSC.
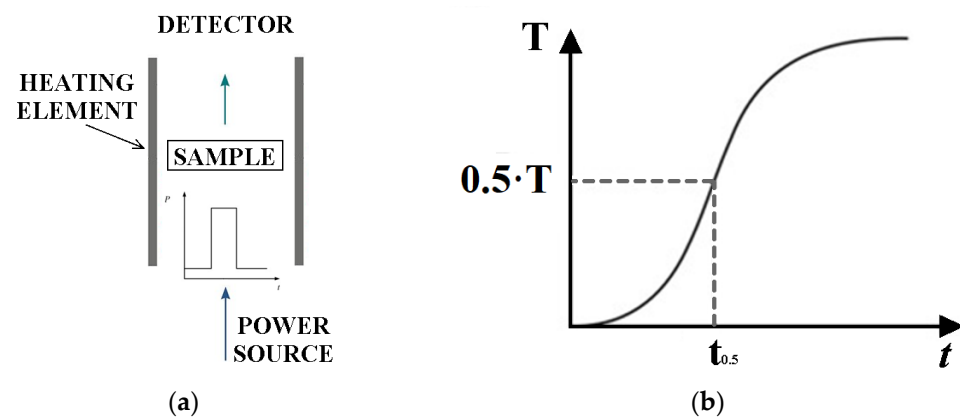
2.3.1. LFA Method

The LFA was developed by Parker in 1961 [29]. This method is commonly used to measure the thermal diffusivity (α), thermal conductivity (k), and specific heat (c_p) of a wide range of solid materials at different temperatures. In the LFA, the bottom surface of a sample is heated by an energy pulse with a certain power and duration. Both the intensity and the duration of the pulse can be adjusted in accordance with the measured sample. The resulting temperature change at the top surface of the sample is then measured with an infrared detector, as shown in Figure 2. The thermal diffusivity of the sample is the relation between the increase in temperature as a function of time, as shown in Equation (2) [30].

$$\alpha = 0.1388 \frac{d^2}{t_{\frac{1}{2}}} \tag{2}$$

where α is the thermal diffusivity in cm^2/s, d is the thickness of the sample in cm, and $t_{\frac{1}{2}}$ is the time for the below surface to reach half of the maximum temperature rise in s (see Figure 2b).

After thermal diffusivity, density (ρ) and specific heat were calculated. These values are used to determine the thermal conductivity of the sample at different temperatures using Equation (3):

$$k(T) = \alpha(T) \times c_p(T) \times \rho(T) \tag{3}$$

Figure 2. LFA method: (**a**) configuration of test; (**b**) calculation of parameters.

The LFA 447 NanoFlash® equipment works according to international standards [31,32], and it was used to perform the experimental campaign. The tested samples were ground concrete particles; consequently, a special sample holder was used to measure thermal conductivity. This sample holder compresses the concrete dust between two layers of aluminum, applying pressure. The thermal conductivity of LWC was measured at temperatures of 100, 220, and 300 °C and pressures of 100, 240, and 290 N/cm² at each temperature. In order to be as close as possible to the porosity conditions of the LWC samples, a series of tests was performed while varying the applied sample pressure.

2.3.2. MTPS Technique

The MTPS technique follows ASTM D7984-16 [33] and employs a one-side, interfacial heat-reflectance sensor that applies a momentary constant heat source to the sample. It causes a rise in temperature at the interface between the sensor and the sample, as shown in Figure 3a. This increase in temperature induces a change in the voltage of the sensor. The rate of increase in the sensor voltage is used to determine the thermo-physical properties of the sample. Thermal conductivity and effusivity are measured directly, providing a detailed overview of the thermal characteristics of the sample. Specific heat is determined using the density of the material (ρ) in kg/m³, the effusivity (E) in Ws$^{1/2}$/m²K, and thermal conductivity (k) in W/mK by means of Equation (4).

$$c_p = \frac{E^2}{k \cdot \rho} \tag{4}$$

In order to measure both k and c_p at different temperatures, 5 × 5 cm cylinder samples were used. The samples were soaked in water for seven days to saturate. Before the samples were heated in a chamber, their thermal conductivity and specific heat were measured at an ambient temperature. Then, the samples were placed in an electronic furnace (MTS 651 Environmental Chamber), as shown in Figure 3b, and they were exposed to a heating curve, as shown in Figure 3c. At 70, 100, 120, and 160 °C, the temperature was kept constant for 50 min. The temperature was increased at a heating rate of 2 °C/min. The change in temperature, as well as the variation in thermal conductivity and the specific heat, were recorded with a sampling frequency of 0.02 Hz by a TCi Thermal Conductivity Analyzer by C-Therm Technologies. All the samples were weighed before and after the test to determine their moisture content.
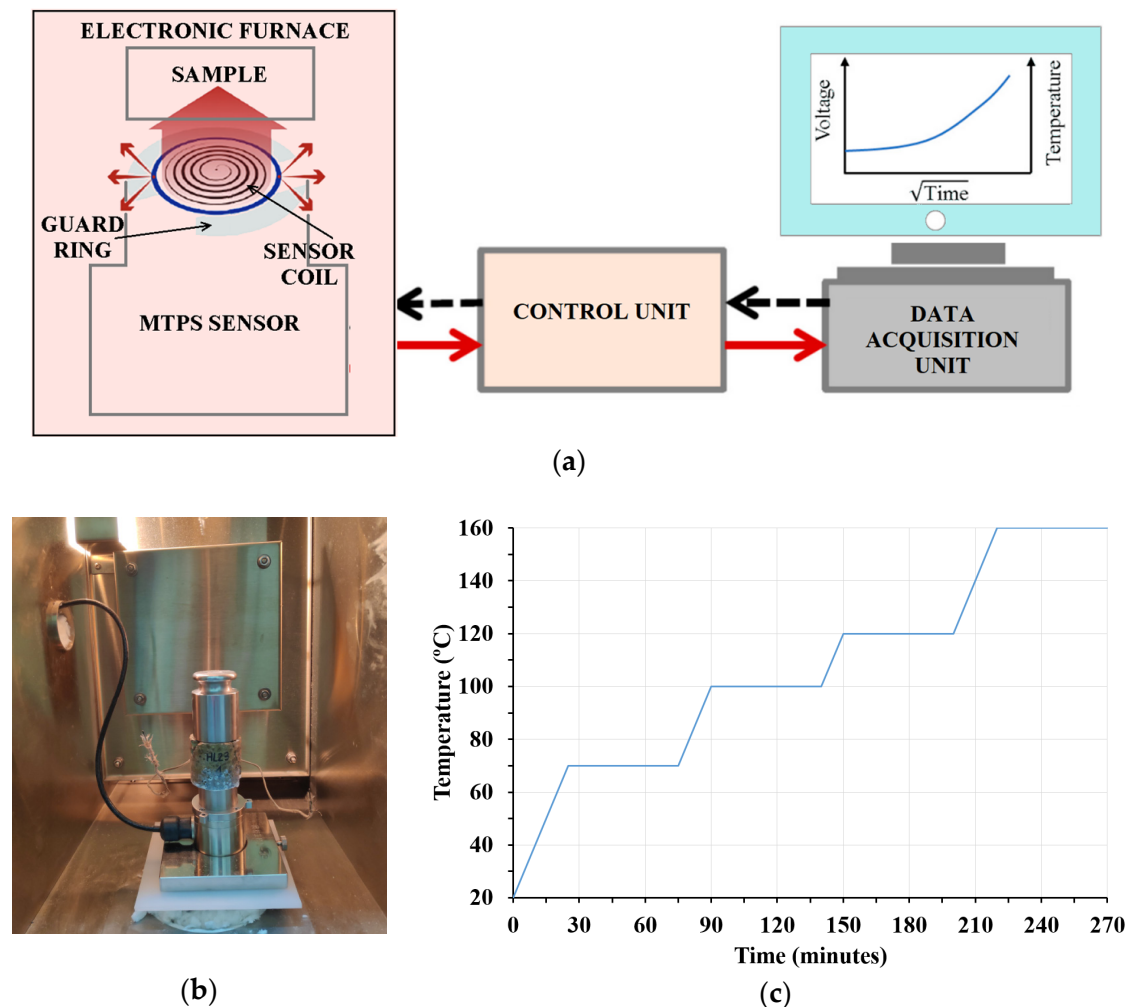
Figure 3. MTPS Test: (**a**) configuration of test; (**b**) placing of the sample in the chamber; (**c**) temperature curve set.

2.3.3. DSC Technique

The DSC technique is a specific type of calorimetry, which uses both a sample material and a reference material. DSC measures the amount of heat required to increase the temperature of a sample and a reference. The reference sample should have a well-defined heat capacity over the range of temperatures to be scanned. The samples and the reference material follow very similar temperature curves throughout the experiment. This method has been widely employed in recent decades for studying phase transitions, such as melting or exothermic decompositions [34–36].

The Netzsch STA 449 F3 equipment is a simultaneous thermal analysis (STA) device based on standards ISO 11358 [37], DIN 51006 [38], and DIN 51007 [39]. It combines thermogravimetry (TG) and differential scanning calorimetry (DSC) in a single test to measure mass change and heat flow as functions of temperature. This equipment was used to determine c_p and perform the experimental campaign. Netzsch STA 449 F3 is able to test in a range of temperature between 30 and 1500 °C in an oxidative or inert atmosphere. The temperature and balance resolutions are 0.001 K and 0.1 µg, respectively, over the entire weighing range. The DSC enthalpy accuracy is ±2% for most materials.

3. Results and Discussion

3.1. LFA Results

In this study, four tests were performed for each LWC using the LFA technique, and the average measurements were also calculated. The thermal conductivity of LWC changes

considerably with the pressure applied. The higher the pressure, the higher its thermal conductivity. A possible explanation for this behavior is the fact that the samples are ground concrete particles. The more pressure is applied, the less air there is in the sample holder, and the higher the thermal conductivity of LWC. Figure 4 shows the relationship between thermal conductivity and pressure for LWC-1. The same behavior was observed for LWC-2 and LWC-3.
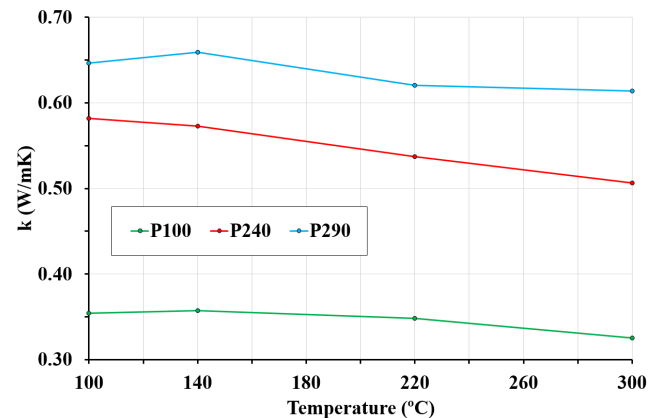

Figure 4. Thermal conductivity for LWC-1 at different pressures (100, 240, and 290 N/cm^2).

Figure 5 shows the average value for the maximum pressure used (290 N/cm^2). Test results for thermal conductivity are given in Figure 5. LWC-3 has the lowest porosity, followed by LWC-2 and LWC-1 (see Table 2). Experimental results with the LFA technique do not provide conclusive results to relate porosity and conductivity. The experimental campaign must be extended to support conclusions.
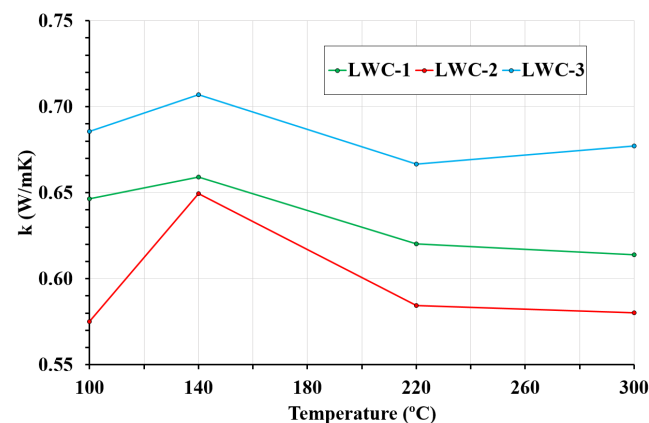

Figure 5. Thermal conductivities for all LWC types.

3.2. MTPS Results

Four tests were performed for each sample block to determine thermal conductivity and specific heat. The average of the four measurements was calculated. The initial moisture content of the LWC samples is calculated using Equation (5). The initial moisture content is between 3% and 8% and, at the end of the tests (160 °C), the moisture content is lower than 1%, which means a reduction in bulk density.

$$MC = \frac{V_{water}}{V_{concrete}} = \left(\frac{m_1 - m_2}{m_1} \right) \times 100 \tag{5}$$

where MC is the percentage of moisture content, m_1 is the mass of the sample at ambient temperature in kg, and m_2 is the mass of the sample in dry conditions in kg.

Thermal conductivity at ambient temperature was measured before starting the heating curve. The results are shown in Table 3. The LWCs studied present high values of porosity, as well as high water content, and they are susceptible to changes in thermal conductivity due to a variation in moisture content [12]. The dependence of LWC thermal conductivity on moisture content is due to the replacement of the air phase by a water phase in the concrete pores. Water-accessible porosity is the key parameter that influences the increase in LWC thermal conductivity with moisture content. In addition, porosity affects thermal conductivity at elevated temperatures; the higher the LWC porosity, the lower its thermal conductivity.

Table 3. Moisture content and average thermal conductivity values of LWC samples at ambient temperature.

Type of Concrete	Sample	Moisture Content (%)	k ($T = 20\,^\circ$C) W/mK
LWC-1	A	3.1 ± 0.1	1.228
LWC-1	B	5.8 ± 0.1	1.596
LWC-1	C	6.2 ± 0.1	1.619
LWC-1	D	6.4 ± 0.1	1.699
LWC-2	A	5.8 ± 0.25	1.499
LWC-2	B	7.4 ± 0.12	1.736
LWC-2	C	7.5 ± 0.1	1.737
LWC-2	D	5.6 ± 0.1	1.470
LWC-3	A	7.3 ± 0.1	1.590
LWC-3	B	6.4 ± 0.1	1.425
LWC-3	C	7.1 ± 0.1	1.562
LWC-3	D	7.6 ± 0.1	1.480

Due to samples having different moisture contents, in this work, a moisture content of 7% was set to study thermal conductivity. According to ISO 10456 [40], a thermal conductivity value related to specific conditions can be transformed to a different value in different conditions. The conversion of thermal values from a set of conditions (k_1) to another set of conditions (k_2) is carried out in accordance with Equation (6) [40]:

$$k_2 = k_1 \times F_T \times F_m \times F_a \tag{6}$$

where k_1 is the thermal conductivity for the first set of conditions (W/mK), k_2 is the thermal conductivity for the second set of conditions (W/mK), F_T is the conversion factor for temperature, F_m is the conversion factor for moisture content, and F_a is the conversion factor for aging.

In the present work, it is assumed that there is no influence from temperature and aging. However, a conversion factor of moisture content was applied, since different moisture content conditions were analyzed. The ISO 10456 establishes a conversion factor (F_{mi}) for the moisture content as a function of the moisture content per unit mass for the i-th set of conditions, u_i, through the conversion coefficient, f_u. Following the research work of del Coz et al. [6], Equation (6) can be transformed into Equation (7).

$$k(\phi) = k_{amb} \times e^{f_u(u_i(\phi) - u_{amb})} \tag{7}$$

where ϕ is the relative humidity, k_{amb} is the thermal conductivity at ambient temperature, f_u is the conversion coefficient of moisture content, u_i is the moisture content for the i conditions, and u_{amb} is the moisture content for ambient conditions.

The conversion of thermal conductivity of LWCs from experimental conditions to reference set conditions is carried out in accordance with Equation (7). Following previous works [6], a conversion coefficient (f_u) of 14 was used for LWC-1, while, for LWC-2 and LWC-3, this value was 6. Least-squares fitting was calculated by minimizing the root-mean-

square error. For a moisture content of 7%, the average thermal conductivity values of LWCs vary from 1.917 to 1.505 W/mK, as shown in Table 4. This is significantly lower than the thermal conductivity of normal concrete. The heat transfer and energy consumption are also lower.

Table 4. Fitted values of thermal conductivity for 7% of moisture content.

Sample	k (LWC-1) W/mK	k (LWC-2) W/mK	k (LWC-3) W/mK
A	2.120	1.611	1.562
B	1.888	1.695	1.477
C	1.811	1.686	1.553
D	1.848	1.599	1.428
Mean value	1.917	1.648	1.505
σ	0.139	0.050	0.064
Error (%)	7.259	3.016	4.243

Figure 6 shows specific heat at elevated temperatures. According to the results, the specific heat behavior of concretes is almost identical for all LWC types. Due to the vaporization of free water in the range of 100 to 140 °C, specific heat increases.

Table 5. Average thermal conductivity values of LWC samples in different high-temperature environments.

Type of Concrete	Sample	k (70 °C) W/mK	k (100 °C) W/mK	k (120 °C) W/mK	k (160 °C) W/mK
LWC-1	A	1.063	1.106	0.902	0.632
LWC-1	B	1.367	1.404	1.100	0.661
LWC-1	C	1.492	1.531	1.127	0.670
LWC-1	D	1.575	1.616	1.253	0.752
Mean value		1.478	1.517	1.160	0.679
Standard deviation		0.225	0.223	0.145	0.051
LWC-2	A	1.348	1.345	1.094	0.791
LWC-2	B	1.704	1.719	1.196	0.819
LWC-2	C	1.630	1.663	1.209	0.828
LWC-2	D	1.408	1.429	1.086	0.827
Mean value		1.522	1.539	1.146	0.816
Standard deviation		0.171	0.181	0.065	0.017
LWC-3	A	1.486	1.503	1.223	0.867
LWC-3	B	1.373	1.380	1.100	0.801
LWC-3	C	1.437	1.537	1.182	0.853
LWC-3	D	1.423	1.495	1.181	0.842
Mean value		1.430	1.479	1.171	0.841
Standard deviation		0.046	0.068	0.052	0.028

The average test results for thermal conductivity at elevated temperatures are shown in Table 5. For all the LWCs, the thermal conductivity behavior is similar, decreasing linearly with temperatures up to 70 °C. It then remains almost constant between 70 and 100 °C, with minor variations attributed to vaporization. Due to the vaporization of free water and the reduction in latent heat, at 100 °C, there is a slight increase in thermal conductivity, as shown in previous works [4,12]. The steep slope of thermal conductivity between 100 and 160 °C can be attributed to moisture loss as a consequence of vaporization of free water with a rise in temperature [12,41]. All the LWCs show thermal conductivity values at elevated temperatures up to 50% lower than at ambient temperature.
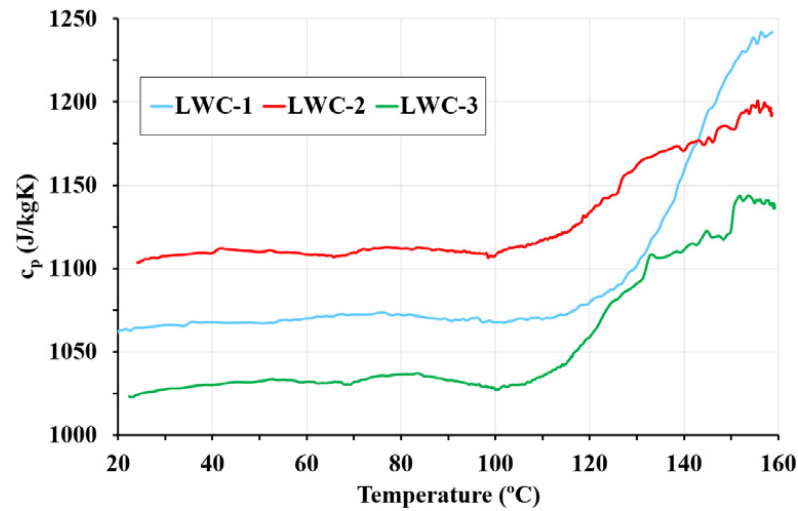
Figure 6. Specific heat for all LWC types.

3.3. DSC Results

Three tests were performed for each sample to determine specific heat. Figure 7 shows the results of specific heat measurements for LWC-1, LWC-2, and LWC-3 at elevated temperatures. It can be seen that all the LWCs follow the same three transition zones, which are related to endothermic peaks, as reported in normal concrete studies [1,4,42]. The first reaction, observed in the temperature range 100–200 °C, is caused by the vaporization of free water within the sample. The second reaction takes place between 400 and 500 °C and is due to the dissociation of calcium hydroxide ($Ca(OH)_2$). Finally, over 800 °C, the dissociation or decomposition of expanded clay occurs [9,21,22]. However, the specific heat curve indicated in Eurocodes 2 and 4 does not take these processes into account. Rather, it simplifies the thermal behavior of lightweight concrete to a constant value.
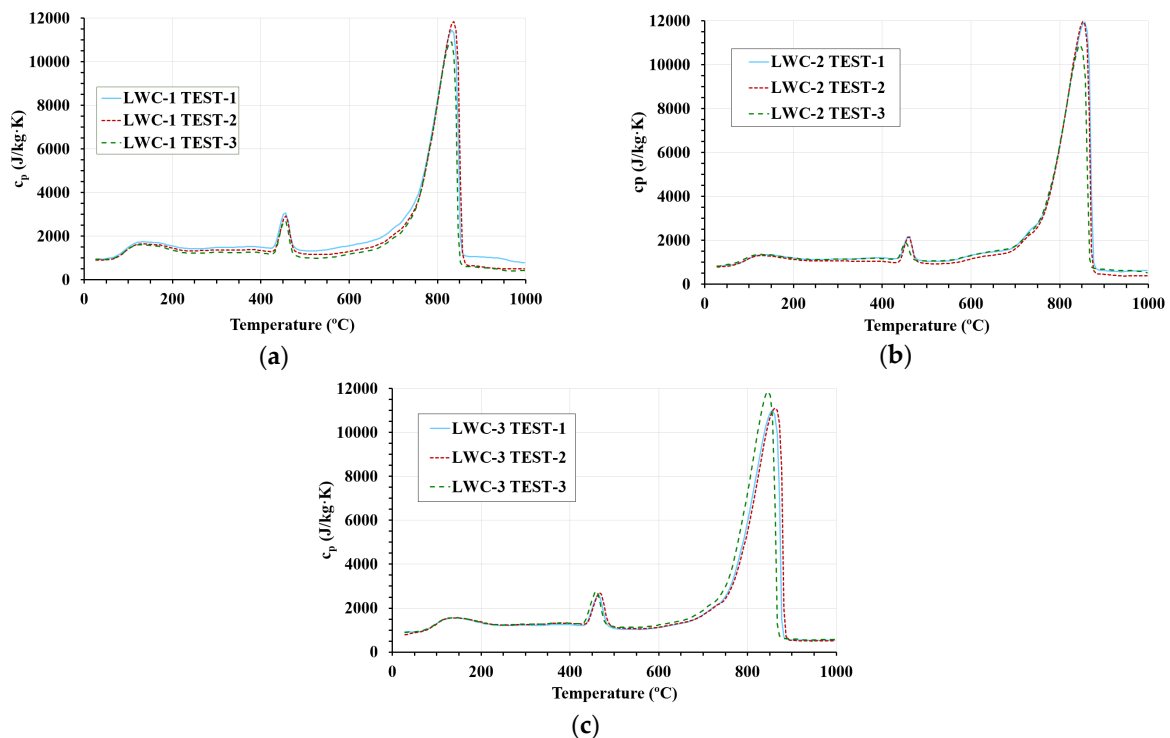

Figure 7. Specific heat for all LWC types: (**a**) LWC-1; (**b**) LWC-2; (**c**) LWC-3.

3.4. Specific Heat

In this research work, two techniques were used to measure specific heat. In both cases, temperature was an influential parameter that affected the specific heat of LWCs. The measured values of specific heat for LWC are higher than those specified in Eurocodes 2 and 4.

The DSC technique provides graphs of specific heat against temperature. Upward peaks indicate endothermic reactions such as vaporization, as shown in Figure 7. However, with the MTPS technique, the specific heat is calculated using a constant value of density. By not taking into account the variation in density (loss of mass), endothermic reactions such as vaporization are not measured. To compare the two techniques, the loss of mass should be measured to provide an adjusted density as a function of temperature. Finally, Equation (4) should be modified to include this adjustment.

To analyze this, after increasing the temperature, the loss of mass was measured using a single-point cell in all the MTPS tests, and the variation in density was calculated. The data were statistically analyzed to generate correlations between the loss of mass and the increase in temperature. The mathematical equation formed through regression analysis is generalized as follows, Equations (8)–(10):

$$\Delta m(T) = -0.0002 \times T + a \quad 20 \leq T \leq 50\,°\text{C} \tag{8}$$

$$\Delta m(T) = -0.00092 \times T + b \quad 50 < T \leq 110\,°\text{C} \tag{9}$$

$$\Delta m(T) = \Delta m(T = 110\,°\text{C}) \quad 110 < T \leq 160\,°\text{C} \tag{10}$$

where $\Delta m(T)$ represents the loss of mass in kg, T is the temperature in $°\text{C}$, and a and b are constants in kg and kg/$°\text{C}$, respectively.

The constants for each LWC, along with the corresponding coefficient of correlation (R^2), are summarized in Table 6. The coefficient of correlation R^2 for all the LWCs studied was more than 0.90, indicating a good correlation between the experimental and calculated data.

Table 6. Coefficients of the fitted curves for loss of mass.

Type of LWC	Coefficients		R^2
LWC-1	a	0.99	0.99
	b	0.9	0.9
LWC-2	a	0.98	0.98
	b	0.91	0.91
LWC-3	a	0.97	0.97
	b	0.94	0.94

Finally, density is calculated as the loss of mass by volume of each sample as a function of temperature. This calculated density is used to determine specific heat, using Equation (4). Figure 8 shows the variation in specific heat in the range of 20–160 °C for the three LWCs studied. Good agreement is found between the calculated and DSC experimental values of specific heat. The modified values of specific heat, plotted with dots, show an increase in specific heat with temperature. The two grey dashed lines represent an error of ±8%. Therefore, the modified specific heat is accurate and able to follow the real behavior of LWCs.
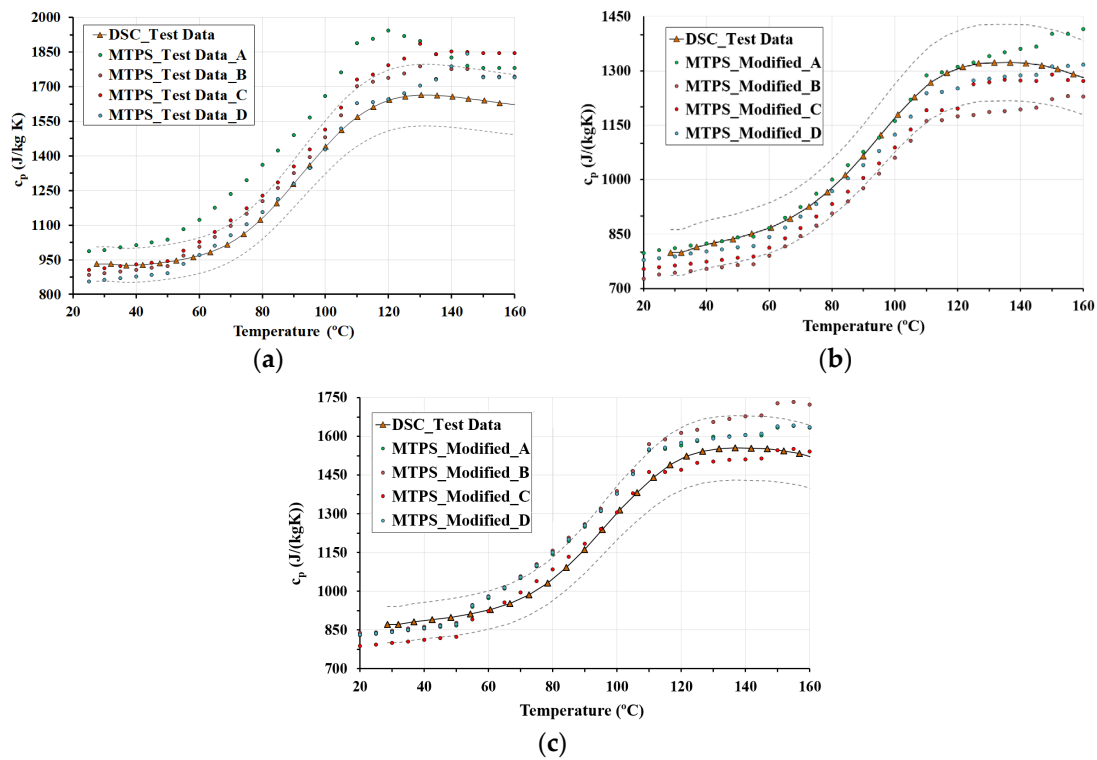
Figure 8. Comparison of specific heat results between 20 and 300 °C: (**a**) LWC-1; (**b**) LWC-2; (**c**) LWC-3.

3.5. Thermal Conductivity

Figure 9 shows the measurement of thermal conductivity in the range of 20–300 °C for the LWCs, studied using LFA and MTPS techniques. Using the MTPS technique, thermal conductivity is measured constantly up to 160 °C, whereas with LFA, thermal conductivity is determined at specific temperatures in the range of 100 to 300 °C.
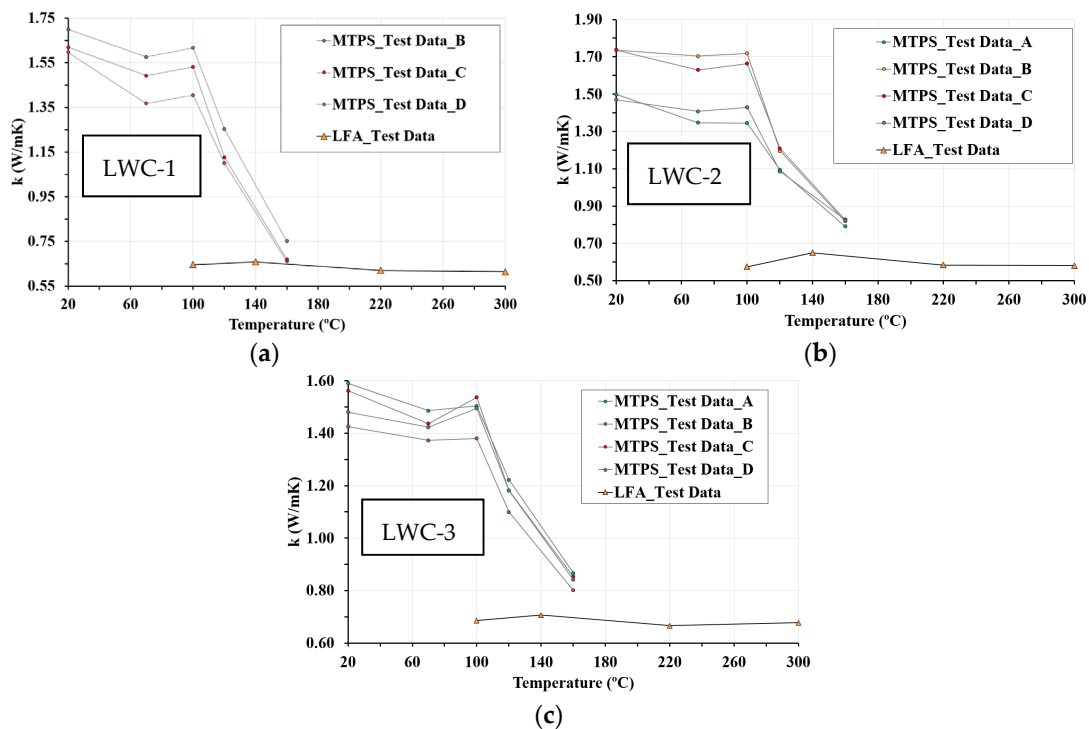

Figure 9. Comparison of thermal conductivity results between 20 and 300 °C: (**a**) LWC-1; (**b**) LWC-2; (**c**) LWC-3.

The results obtained by the two techniques at 100 °C differ due to the moisture content of the samples, which are dehydrated in order to use them in the LFA equipment. Although the water losses do not correspond with one another, the measurements at the additional points of 220 and 300 °C are similar. The MTPS technique reflects the dehydration process up to 140 °C and the consequent decrease in the value of the thermal conductivity of the material. Free water starts to evaporate at 100 to 120 °C. The presence of pores within the lightweight concrete accelerates this phenomenon. Therefore, the dehydration process associated with the reduction in moisture content causes a pronounced drop in thermal conductivity. Above this temperature, at which there is practically no water in the concrete, the values obtained by means of LFA can be considered valid. The two techniques are complementary, as shown by the continuity of the thermal conductivity values at 140 °C and represented in Figure 9.

4. Proposed Thermal Properties Relationships

Thermal properties of LWC are commonly used as input data to solve heat transfer analysis. In the current study, thermal relationships were developed. Step-by-step formulae, similar to those in Eurocodes 2 and 4, are presented in the following sections.

4.1. Specific Heat Equations

Data generated from the specific heat measurements are used to develop a specific heat relationship for LWC. This thermal property is expressed in the form of an empirical relationship in the temperature range of 20–1000 °C, as shown in Figure 10a. The accuracy of the statistical model is represented by the coefficient of determination, R^2, whose value lies between 0.9 and 0.97.
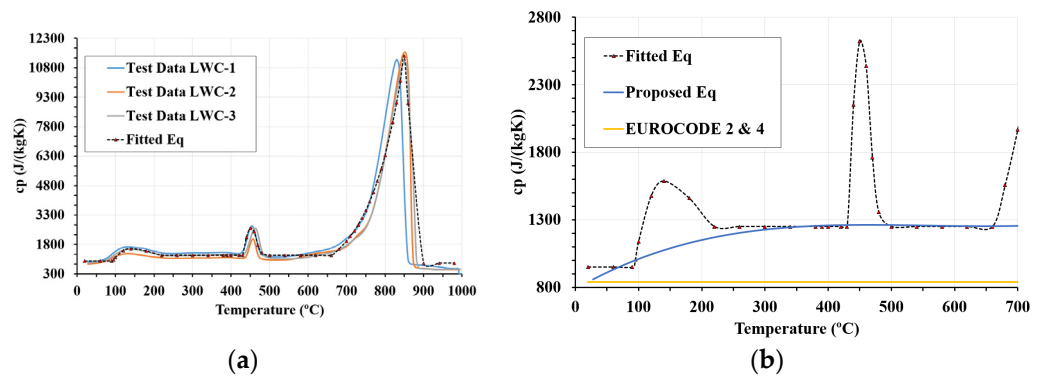
Figure 10. Specific heat: (**a**) comparison of the experimental and proposed specific heat equations; (**b**) comparison of proposed equations, simplified equation, and Eurocodes 2 and 4 values.

Specific heat is mainly influenced by the temperature range. To capture this trend, several equations are proposed. These relationships are presented in Equation (11) through Equation (19) in J/kg°C.

$$c_p(T) = 950 \qquad\qquad 20 \leq T \leq 100\ °C \quad (11)$$

$$c_p(T) = 0.0018\left[\frac{J}{\text{kg}°\text{C}^4}\right] \times T^3 - 0.9352\left[\frac{J}{\text{kg}°\text{C}^3}\right] \times T^2 + 157.16\left[\frac{J}{\text{kg}°\text{C}^2}\right] \times T - 7025.4\left[\frac{J}{\text{kg}°\text{C}}\right]\ (R^2 = 0.96) \qquad 100 < T \leq 200\ °C \quad (12)$$

$$c_p(T) = 1250 \qquad\qquad 200 < T \leq 430\ °C \quad (13)$$

$$c_p(T) = -0.0069\left[\frac{J}{\text{kg}°\text{C}^4}\right] \times T^3 + 9.8164\left[\frac{J}{\text{kg}°\text{C}^3}\right] \times T^2 - 4590.3\left[\frac{J}{\text{kg}°\text{C}^2}\right] \times T + 709,200\left[\frac{J}{\text{kg}°\text{C}}\right]\ (R^2 = 0.97) \qquad 430 < T \leq 450\ °C \quad (14)$$

$$c_p(T) = 1.3695\left[\frac{J}{\text{kg}°\text{C}^3}\right] \times T^2 - 1341.5\left[\frac{J}{\text{kg}°\text{C}^2}\right] \times T + 329,744\left[\frac{J}{\text{kg}°\text{C}}\right]\ (R^2 = 0.97) \qquad 450 < T \leq 500\ °C \quad (15)$$

$$c_p(T) = 1250 \qquad\qquad 500 < T \leq 650\ °C \quad (16)$$

$$c_p(T) = 0.5463 \cdot e^{0.0117 \times T} \ (R^2 = 0.95) \qquad\qquad 650 < T \leq 850\ ^\circ\text{C} \qquad (17)$$

$$c_p(T) = -208.51\left[\tfrac{J}{\text{kg}^\circ\text{C}^2}\right] \times T + 185{,}723\left[\tfrac{J}{\text{kg}^\circ\text{C}}\right]\ (R^2 = 0.91) \qquad\qquad 850 < T < 900\ ^\circ\text{C} \qquad (18)$$

$$c_p(T) = 850 \qquad\qquad 900 \leq T \leq 1000\ ^\circ\text{C} \qquad (19)$$

The current Eurocodes 2 and 4 for evaluating the fire resistance of concrete elements assume that specific heat for normal concrete can be simplified with an equation as a function of temperature. However, for LWC, this assumption has numerous drawbacks. For LWC, Eurocodes 2 and 4 propose a constant value (840 J/kg°C). In this research work, to fit a specific heat equation to LWC, the following equation is presented for the temperature range of 20–700 °C:

$$c_p(T) = 3 \cdot 10^{-6}\left[\frac{J}{\text{kg}^\circ\text{C}^4}\right] \times T^3 - 0.005\left[\frac{J}{\text{kg}^\circ\text{C}^3}\right] \times T^2 + 2.7\left[\frac{J}{\text{kg}^\circ\text{C}^2}\right] \times T + 786\left[\frac{J}{\text{kg}^\circ\text{C}}\right] \qquad (20)$$

where $c_p(T)$ is the specific heat of LWC as a function of temperature and T is the temperature in °C.

Figure 10b shows the comparison between the fitted equation, the proposed equation, and the Eurocodes. The Eurocodes underestimate the specific heat of LWC. However, the trendline for proposed values from the current study is close to the line depicting results without taking into account the peaks caused by the vaporization of free water, the dissociation of calcium hydroxide, and the dissociation or decomposition of expanded clay.

4.2. Thermal Conductivity Equations

Data generated from the thermal conductivity measurements are used to develop thermal conductivity relationships for LWC. This thermal property is expressed in the form of empirical relationships in the temperature range of 20–300 °C. A good relation was found between the experimental and the statistical model, as noted by R^2, whose value lay between 0.9 and 1.

The test data clearly indicate that thermal conductivity is mainly influenced by the porosity of LWC and the temperature range. To reflect this trend, separate expressions are developed for thermal conductivity. Thermal conductivity relationships are presented in three temperature ranges: 20–100, 100–180, and 180–300 °C. These relations are presented in Equations (21)–(23):

$$k(T) = \rho_{20^\circ\text{C}} \times \left(9.4 \cdot 10^{-4}\left[\tfrac{\text{Wm}^2}{\text{kg}^\circ\text{C}}\right] - 10^{-6}\left[\tfrac{\text{Wm}^2}{\text{kg}^\circ\text{C}^2}\right] \times T(^\circ\text{C})\right) \ (R^2 = 0.9) \qquad\qquad 20 \leq T < 100\ ^\circ\text{C} \qquad (21)$$

$$k(T) = \rho_{20^\circ\text{C}} \times \left(\tfrac{e^{-0.01 \times T(^\circ\text{C})}}{425}\right) \ (R^2 = 0.97) \qquad\qquad 100 \leq T < 180\ ^\circ\text{C} \qquad (22)$$

$$k(T) = \rho_{20^\circ\text{C}} \times \left(-3 \cdot 10^{-7}\left[\tfrac{\text{Wm}^2}{\text{kg}^\circ\text{C}^2}\right] \times T(^\circ\text{C}) - 4.5 \cdot 10^{-4}\left[\tfrac{\text{Wm}^2}{\text{kg}^\circ\text{C}}\right]\right) \ (R^2 = 0.95) \qquad\qquad 180 \leq T < 300\ ^\circ\text{C} \qquad (23)$$

where $k(T)$ is the thermal conductivity of LWC as a function of temperature, $\rho_{20^\circ\text{C}}$ is the density of LWC at 20 °C, and T is the temperature in °C.

Figure 11 shows the comparison between the experimental data, the fitted equation, and Eurocodes. Eurocodes underestimate thermal conductivity of LWC up to 150 °C. However, above 150 °C, Eurocodes overestimate this thermal property. The trendline for the fitted equation is close to the line depicting results from MTPS data and LFA data.
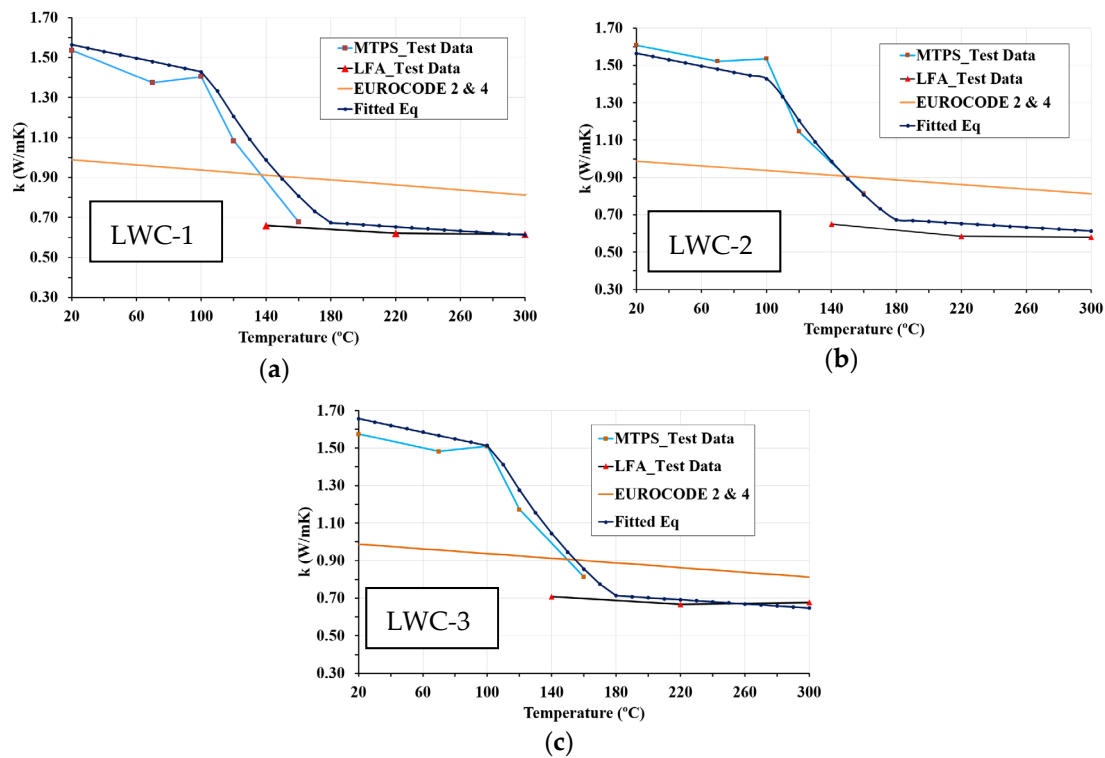
Figure 11. Comparison of the experimental and proposed thermal conductivity: (**a**) LWC-1; (**b**) LWC-2; (**c**) LWC-3.

5. Conclusions

This research focuses on the thermal properties of three types of structural lightweight concrete. In order to study specific heat and thermal conductivity, three techniques were used. The main conclusions of this work can be summarized in the three sections below:

1. General conclusions:

    i. Porosity and bulk density of LWCs show an inverse relationship at low temperatures: the higher the porosity, the lower the bulk density. LWC-1 has the highest porosity, 28%, and the lowest bulk density, 1740 kg/m^3. True density is defined as the relationship between the mass and volume of the concrete, including the pores in the material. Taking into account this relationship, the true density of the three LWCs is similar: between 1.3 and 1.4 times higher than the bulk density.

    ii. The structural LWCs studied have significantly lower thermal conductivity than normal concrete, reducing heat losses. Thermal conductivity of LWC is highly affected by moisture content, which depends on porosity and temperature. In this sense, at low temperatures, the higher the porosity, the higher the thermal conductivity; however, at high temperatures, the higher the porosity is, the lower the thermal conductivity is. The results of the tests reveal this variability in the thermal conductivity of LWCs.

    iii. This research shows interesting differences in the performance of samples manufactured with different dosages of aggregates. This demonstrates the importance of a preliminary phase of material characterization. The standard ISO10456 must be updated to adapt the conversion coefficients when expanded clay is used as the main aggregate. This research work proposes a conversion factor between 6 and 14 for all the LWC mixes with densities between 1700 and 1900 kg/m^3.

    iv. The current Eurocodes 2 and 4 used for evaluating the fire resistance of elements assume that specific heat for LWC can be simplified with a constant value of 840 J/kg°C. However, the results of this research work sug-

gest a change to the Eurocodes as temperature has a significant influence on specific heat.

2. Thermal techniques:

    i.   The results of this work show the efficiency of combining MTPS and LFA techniques to measure thermal conductivity in a wide temperature range. The MTPS technique measures thermal conductivity from ambient temperature up to 160 °C. Although LFA tests with ground particles have inherent limitations due to parti-cle contact, above 160 °C, at which there is practically no water in the concrete, the values obtained by LFA could be considered valid. Both techniques are complementary, as demonstrated by the equality of the thermal conductivity values at 160 °C. The MTPS technique requires a stabilization time longer than 1 h to reduce the moisture content of the samples.

    ii. The MTPS and DSC techniques show that temperature is an influential parameter and must be taken into account to calculate the specific heat. Both techniques show that the specific heat for LWC is higher than the values specified in Eurocodes 2 and 4. Specific heat is affected by decomposition reactions, as shown in the DSC results. For this reason, the MTPS technique should take into account the loss of mass caused by water vaporization to provide an adjusted value of specific heat. Therefore, in order to use the MTPS technique to obtain an adjusted value of the specific heat at elevated temperatures, the density of the material must be measured as a function of the test temperature, and Equation (4) should be applied to make the corresponding adjustments.

3. Proposed equations:

    i.   The proposed equations for specific heat are based on experimental data and dependent on temperature and fitting the experimental values. Although Eurocodes 2 and 4 assume a constant value for specific heat, this research work shows that this assumption has numerous drawbacks. From the assumption of Eurocodes 2 and 4 for normal concrete, an equation is proposed for the temperature range of 20–700 °C. This proposed equation fits the experimental values more accurately.

    ii. The proposed equations for thermal conductivity, based on experimental data, depend on the temperature and density of LWCs. These simplified relations for high-temperature thermal properties of new types of concrete are adequate for incorporation in codes and standards. In addition, these formulae can be used as input for numerical models, which can be used to determine the behavior of LWC structural elements at elevated temperatures.

The findings of this study constitute a realistic characterization of the thermal conductivity and specific heat of LWCs in different temperature ranges, combining the results of different measurement techniques. The research concludes that the specific heat of LWC must not be considered constant as standards establish.

Further investigation should be conducted on different types of LWC with different densities to determine the effectiveness of the proposed equations.

Author Contributions: Conceptualization, J.J.d.C.-D.; methodology, F.P.Á.R.; validation, F.P.Á.R. and M.L.; formal analysis, J.E.M.-M.; investigation, M.L.; data curation, J.E.M.-M.; writing—original draft preparation, J.E.M.-M.; writing—review and editing, M.A.-M.; visualization, J.E.M.-M.; supervision, D.A.; funding acquisition, J.J.d.C.-D. All authors have read and agreed to the published version of the manuscript.

Institutional Review Board Statement: Not applicable.

Informed Consent Statement: Not applicable.

Data Availability Statement: Data are available on request.

Conflicts of Interest: The authors declare no conflict of interest. The funders had no role in the design of the study; in the collection, analyses, or interpretation of data; in the writing of the manuscript, or in the decision to publish the results.

References

1. Venkatesh, K. Properties of Concrete at Elevated Temperatures. *ISRN Civ. Eng.* **2014**, *2014*, 15. [CrossRef]
2. Zhou, H.; Brooks, A.L. Thermal and mechanical properties of structural lightweight concrete containing lightweight aggregates and fly-ash cenospheres. *Constr. Build. Mater.* **2019**, *198*, 512–526. [CrossRef]
3. Chalangaran, N.; Farzampour, A.; Paslar, N. Nano Silica and Metakaolin Effects on the Behavior of Concrete Containing Rubber Crumbs. *CivilEng* **2020**, *1*, 264–274. [CrossRef]
4. Yun, T.S.; Jeong, Y.J.; Youm, K.-S. Effect of Surrogate Aggregates on the Thermal Conductivity of Concrete at Ambient and Elevated Temperatures. *Sci. World J.* **2014**, *2014*, 1–9. [CrossRef]
5. *Transition to Sustainable Buildings: Strategies and Opportunities to 2050*; OECD: Paris, France, 2013. [CrossRef]
6. del Coz Díaz, J.J.; Álvarez Rabanal, F.P.; García Nieto, P.J.; Domínguez Hernández, J.; Rodríguez Soria, B.; Pérez-Bella, J.M. Hygrothermal properties of lightweight concrete: Experiments and numerical fitting study. *Constr. Build. Mater.* **2013**, *40*, 543–555. [CrossRef]
7. Gencel, O.; del Coz Díaz, J.J.; Sutcu, M.; Kocyigit, F.; Rabanal, F.P.Á.; Alonso-Martínez, M.; Barrera, G.M. Thermal Performance Optimization of Lightweight Concrete/EPS Layered Composite Building Blocks. *Int. J. Thermophys.* **2021**, *42*, 52. [CrossRef]
8. del Coz Díaz, J.J.; Álvarez-Rabanal, F.P.; Alonso-Martínez, M.; Martínez-Martínez, J.E. Thermal Inertia Characterization of Multilayer Lightweight Walls: Numerical Analysis and Experimental Validation. *Appl. Sci.* **2021**, *11*, 5008. [CrossRef]
9. Lie, T.T.; Kodur, V.K.R. Thermal and mechanical properties of lightweight foamed concrete at elevated temperatures. *Mag. Concr. Res.* **1996**, *23*, 511–517. [CrossRef]
10. Burbano-Garcia, C.; Hurtado, A.; Silva, Y.F.; Delvasto, S.; Araya-Letelier, G. Utilization of waste engine oil for expanded clay aggregate production and assessment of its influence on lightweight concrete properties. *Constr. Build. Mater.* **2021**, *273*, 121677. [CrossRef]
11. Shoukry, S.N.; William, G.W.; Downie, B.; Riad, M.Y. Effect of moisture and temperature on the mechanical properties of concrete. *Constr. Build. Mater.* **2011**, *25*, 688–696. [CrossRef]
12. Al-Sibahy, A.; Edwards, R. Thermal behaviour of novel lightweight concrete at ambient and elevated temperatures: Experimental, modelling and parametric studies. *Constr. Build. Mater.* **2012**, *31*, 174–187. [CrossRef]
13. Nguyen, L.H.; Beaucour, A.L.; Ortola, S.; Noumowé, A. Experimental study on the thermal properties of lightweight aggregate concretes at different moisture contents and ambient temperatures. *Constr. Build. Mater.* **2017**, *151*, 720–731. [CrossRef]
14. Asadi, I.; Shafigh, P.; Hassan, Z.F.B.A.; Mahyuddin, N.B. Thermal conductivity of concrete—A review. *J. Build. Eng.* **2018**, *20*, 81–93. [CrossRef]
15. Khaliq, W.; Kodur, V. High temperature mechanical properties of high-strength fly ash concrete with and without fibers. *ACI Mater. J.* **2012**, *109*, 665–674. [CrossRef]
16. Davie, C.T.; Pearce, C.J.; Bićanić, N. Coupled heat and moisture transport in concrete at elevated temperatures—Effects of capillary pressure and adsorbed water. *Numer. Heat Transf. Part A Appl.* **2006**, *49*, 733–763. [CrossRef]
17. *UNE-EN 1992-1-2 Eurocode 2: Design of Concrete Structures—Part 1-2: General Rules—Structural Fire Design*; AENOR: Madrid, Spain, 2011.
18. *UNE-EN 1994-1-2 Eurocode 4—Design of Composite Steel and Concrete Structures—Part 1-2: General Rules—Structural Fire Design*; AENOR: Madrid, Spain, 2016.
19. Kodur, V.K.R.; Sultan, M.A. Effect of Temperature on Thermal Properties of High-Strength Concrete. *J. Mater. Civ. Eng.* **2003**, *15*, 101–107. [CrossRef]
20. Adl-Zarrabi, B.; Boström, L.; Wickström, U. Using the TPS method for determining the thermal properties of concrete and wood at elevated temperature. *Fire Mater.* **2006**, *30*, 359–369. [CrossRef]
21. Othuman, M.A.; Wang, Y.C. Elevated-temperature thermal properties of lightweight foamed concrete. *Constr. Build. Mater.* **2011**, *25*, 705–716. [CrossRef]
22. Alarcon-Ruiz, L.; Platret, G.; Massieu, E.; Ehrlacher, A. The use of thermal analysis in assessing the effect of temperature on a cement paste. *Cem. Concr. Res.* **2005**, *35*, 609–613. [CrossRef]
23. Yu, Q.L.; Spiesz, P.; Brouwers, H.J.H. Ultra-lightweight concrete: Conceptual design and performance evaluation. *Cem. Concr. Compos.* **2015**, *61*, 18–28. [CrossRef]
24. Kodur, V.K.R.; Banerji, S.; Solhmirzaei, R. Test methods for characterizing concrete properties at elevated temperature. *Fire Mater.* **2020**, *44*, 381–395. [CrossRef]

25. *UNE-EN 197-1 Cement—Part 1: Composition, Specifications and Conformity Criteria for Common Cements*; AENOR: Madrid, Spain, 2011.

26. UNE 83502:2004. *Concrete with Fibers. Method of Making in the Laboratory*; AENOR: Madrid, Spain, 2004.

27. UNE 83504:2004. *Concrete with Fibers. Making and Maintenance of Specimens for Laboratory Tests*; AENOR: Madrid, Spain, 2004.

28. Wu, A.; Wang, Y.; Wang, H. Estimation model for yield stress of fresh uncemented thickened tailings: Coupled effects of true solid density, bulk density, and solid concentration. *Int. J. Miner. Process.* **2015**, *143*, 117–124. [CrossRef]

29. Parker, W.J.; Jenkins, R.J.; Butler, C.P.; Abbott, G.L. Flash method of determining thermal diffusivity, heat capacity, and thermal conductivity. *J. Appl. Phys.* **1961**, *32*, 1679–1684. [CrossRef]

30. *NETZSCH, Laser Flash Analysis—LFA, Produktfolder LFA 427*; ASTM International: West Conshohocken, PA, USA, 2013.

31. ASTM International. *ASTM Standard E1461−13. Standard Test Method for Thermal Diffusivity by the Flash Method*; ASTM International: West Conshohocken, PA, USA, 2013.

32. ISO 22007-4:2017. *Plastics—Determination of Thermal Conductivity and Thermal Diffusivity—Part 4: Laser Flash Method*; ISO: Geneva, Switzerland, 2017.

33. *ASTM D7984—16 Standard Test Method for Measurement of Thermal Effusivity of Fabrics Using a Modified Transient Plane Source (MTPS) Instrument*; ASTM International: West Conshohocken, PA, USA, 2016.

34. Seng, B.; Magniont, C.; Lorente, S. Characterization of a precast hemp concrete. Part I: Physical and thermal properties. *J. Build. Eng.* **2019**, *24*, 100540. [CrossRef]

35. Li, B.; Mao, J.; Nawa, T.; Han, T. Mesoscopic damage model of concrete subjected to freeze-thaw cycles using mercury intrusion porosimetry and differential scanning calorimetry (MIP-DSC). *Constr. Build. Mater.* **2017**, *147*, 79–90. [CrossRef]

36. Romano, A.; Grammatikos, S.; Riley, M.; Bras, A. Determination of specific heat capacity of bio-fibre earth mortars stabilised at different relative humidities using Differential Scanning Calorimetry. *J. Build. Eng.* **2021**, *41*, 102738. [CrossRef]

37. ISO 11358-1:2014. *Plastics—Thermogravimetry (TG) of Polymers—Part 1: General Principles*; ISO: Geneva, Switzerland, 2014.

38. DIN 51006:2005-07. *Thermal Analysis (TA)-Thermogravimetry (TG)—Principles*; Deutsches Institut für Normung e.V: Berlin, Germany, 2015.

39. DIN 51007:2019-04. *Thermal Analysis—Differential Thermal Analysis (DTA) and Differential Scanning Calorimetry (DSC)—General Principles*; Deutsches Institut für Normung e.V: Berlin, Germany, 2019.

40. ISO 10456:2007. *Building Materials and Products—Hygrothermal Properties—Tabulated Design Values and Procedures for Determining Declared and Design Thermal Values*; ISO: Geneva, Switzerland, 2007.

41. Kodur, V.; Khaliq, W. Effect of Temperature on Thermal Properties of Different Types of High-Strength Concrete. *J. Mater. Civ. Eng.* **2011**, *23*, 793–801. [CrossRef]

42. Gad, E.A.M.; Habib, A.O.; Mousa, M.M. Understanding the mechanism of decomposition reactions of neat and superplasticized ordinary Portland cement pastes using thermal analysis. *Epa.-J. Silic. Based Compos. Mater.* **2018**, *70*, 98–103. [CrossRef]